

Electronic Supplementary Information

Functionalized phenylimidazole-based *facial*-homoleptic iridium(III) complexes and their excellent performance in blue phosphorescent organic light-emitting diodes

Youngjae Kwon,^{‡a} Si Hyun Han,^{‡b} Seokhyeon Yu^a, Jun Yeob Lee^{*b} and Kang Mun Lee^{*a}

^a *Department of Chemistry, Institute for Molecular Science and Fusion Technology, Kangwon National University, Chuncheon, Gangwon 24341, Republic of Korea*

^b *School of Chemical Engineering, Sungkyunkwan University, 2066, Seobu-ro, Jangan-gu, Suwon, Gyeonggi 16419, Republic of Korea*

[‡] *The first, second, and third authors contributed equally to this work*

**E-mail: leej17@skku.edu*

**E-mail: kangmunlee@kangwon.ac.kr*

Table S1 Crystallographic data and parameters for **FIr** and **CNIr**

Compound	FIr ·(<i>n</i> -hexane)	CNIr
Formula	C ₆₉ H ₈₀ F ₃ IrN ₆	C ₆₆ H ₆₆ IrN ₉
Formula weight	1242.59	1177.47
Crystal system	Monoclinic,	Monoclinic
Space group	<i>P2(1)/n</i>	<i>P2(1)/n</i>
<i>a</i> (Å)	13.994(3)	14.985(3)
<i>b</i> (Å)	21.759(4)	26.651(5)
<i>c</i> (Å)	23.610(5)	17.246(3)
α (°)	90	90
β (°)	97.437(8)	102.60(3)
γ (°)	90	90
<i>V</i> (Å ³)	7129(2)	6721(2)
<i>Z</i>	4	4
ρ_{calc} (g cm ⁻³)	1.158	1.164
μ (mm ⁻¹)	1.920	2.028
<i>F</i> (000)	2560	2408
<i>T</i> (K)	223(2)	293(2) K 2.068 to 28.356°.
Scan mode	<i>multi</i>	<i>multi</i>
<i>hkl</i> range	-18 → +18, -29 → +28, -31 → +31	-20 → +20, -35 → +35, -23 → +21
Measd reflns	235130	247154
Unique reflns [<i>R</i> _{int}]	17785 [0.0807]	16757 [0.1033]
Reflns used for refinement	17785	16757
Refined parameters	726	697
<i>R</i> ₁ ^{<i>a</i>} (<i>I</i> > 2σ(<i>I</i>))	0.0429	0.0463
w <i>R</i> ₂ ^{<i>b</i>} all data	0.1081	0.1544
GOF on <i>F</i> ²	1.025	1.021
ρ_{fin} (max/min) (e Å ⁻³)	0.683, -0.353	0.810, -0.715

^{*a*} $R_1 = \sum ||F_o| - |F_c| / \sum |F_o|$. ^{*b*} $wR_2 = \{[\sum w(F_o^2 - F_c^2)^2] / [\sum w(F_o^2)^2]\}^{1/2}$.

Table S2 Selected bond lengths (Å) and angles (°) for **FIr** and **CNIr**

FIr		CNIr	
lengths (Å)			
Ir–C1	2.020(3)	Ir–C1	2.017(5)
Ir–C22	2.009(3)	Ir–C22	2.011(5)
Ir–C43	2.017(3)	Ir–C43	2.013(5)
Ir–N1	2.111(3)	Ir–N1	2.125(4)
Ir–N3	2.114(3)	Ir–N3	2.116(4)
Ir–N5	2.108(3)	Ir–N5	2.094(4)
angles (°)			
C1–Ir–C22	94.78(12)	C1–Ir–C22	96.21(18)
C1–Ir–C43	93.87(12)	C1–Ir–C43	95.03(18)
C22–Ir–C43	94.53(13)	C22–Ir–C43	94.64(19)
C1–Ir–N5	171.27(11)	C1–Ir–N5	88.56(17)
C22–Ir–N5	91.40(11)	C22–Ir–N5	172.86(17)
C43–Ir–N5	79.47(11)	C43–Ir–N5	79.61(18)
C1–Ir–N1	79.13(11)	C1–Ir–N1	79.28(17)
C22–Ir–N1	173.26(11)	C22–Ir–N1	94.17(17)
C43–Ir–N1	88.82(12)	C43–Ir–N1	169.98(18)
C1–Ir–N3	93.38(11)	C1–Ir–N3	174.31(18)
C22–Ir–N3	79.14(11)	C22–Ir–N3	79.22(17)
C43–Ir–N3	170.74(11)	C43–Ir–N3	88.76(18)
N1–Ir–N3	98.19(10)	N1–Ir–N3	97.56(16)
N1–Ir–N5	94.96(10)	N1–Ir–N5	91.93(16)
N3–Ir–N5	93.83(10)	N3–Ir–N5	96.31(17)

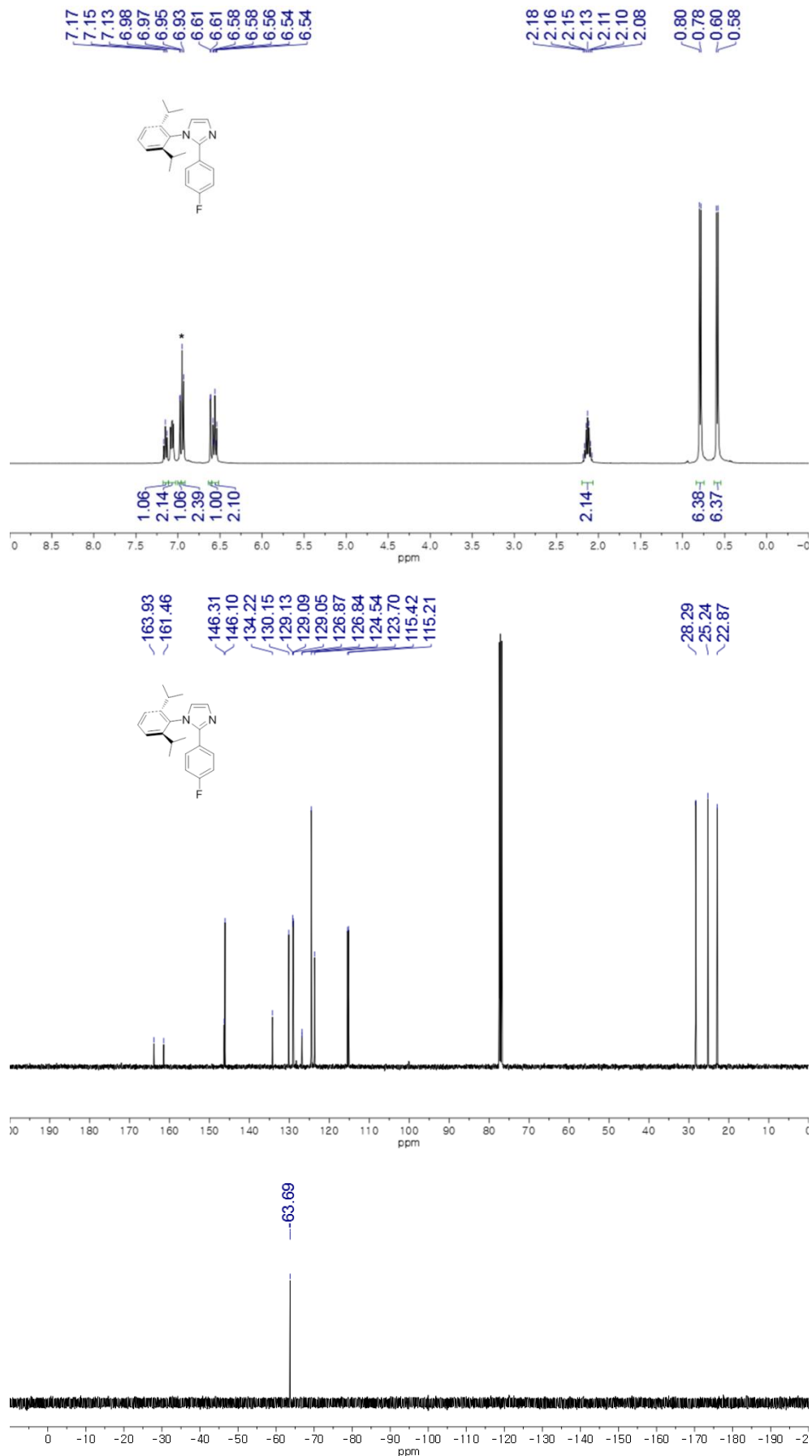


Fig. S1 ¹H (top), ¹³C (middle) and ¹⁹F NMR spectrum of **FL** (* from residual CHCl₃ in CDCl₃).

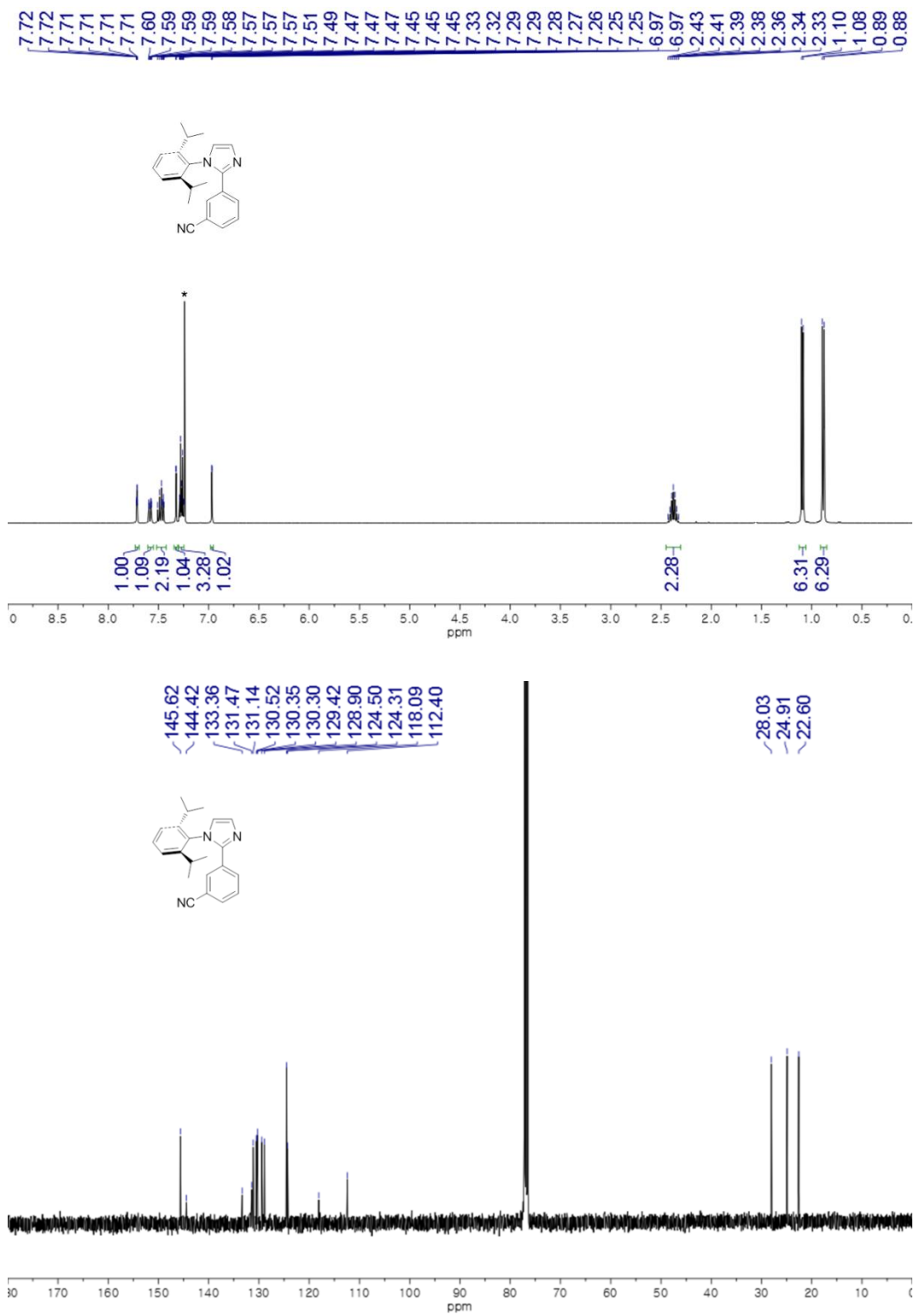


Fig. S2 ¹H (top) and ¹³C (bottom) NMR spectrum of CNL (* from residual CHCl₃ in CDCl₃).

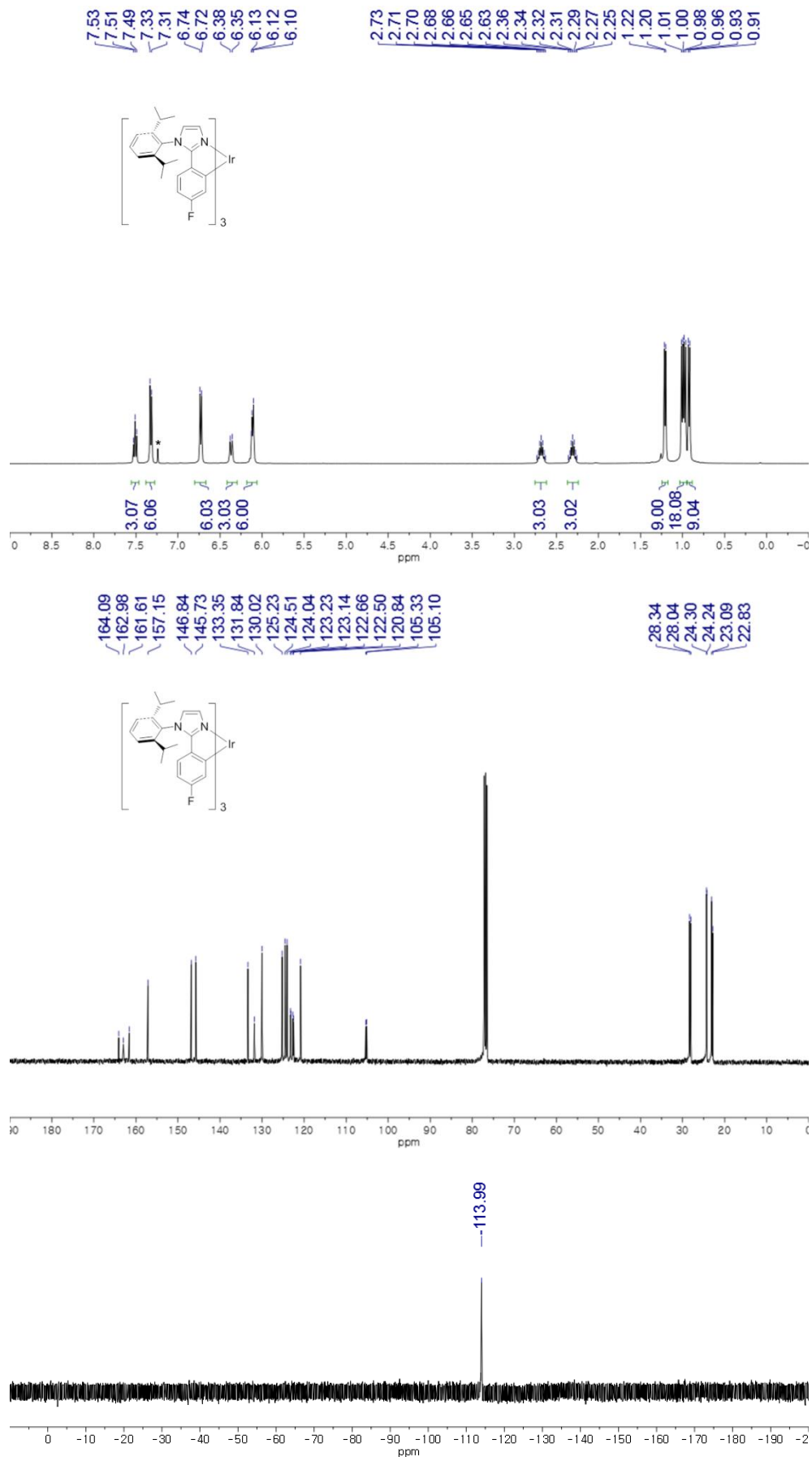


Fig. S3 ¹H (top), ¹³C (middle) and ¹⁹F NMR spectrum of *fac*-**FIr** (* from residual CHCl₃ in CDCl₃).

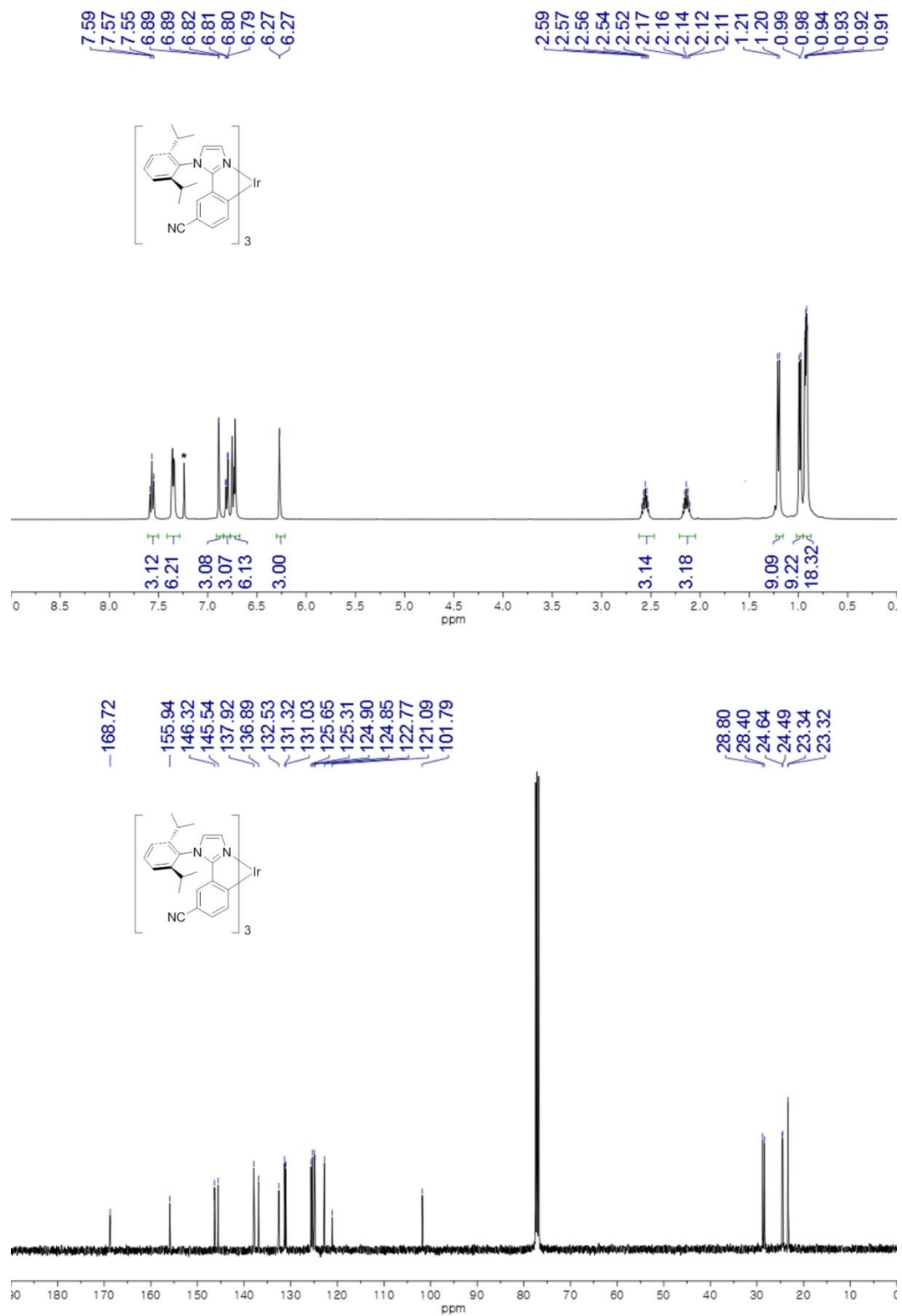


Fig. S4 ¹H (top) and ¹³C (bottom) NMR spectrum of *fac*-CNIr (* from residual CHCl₃ in CDCl₃).

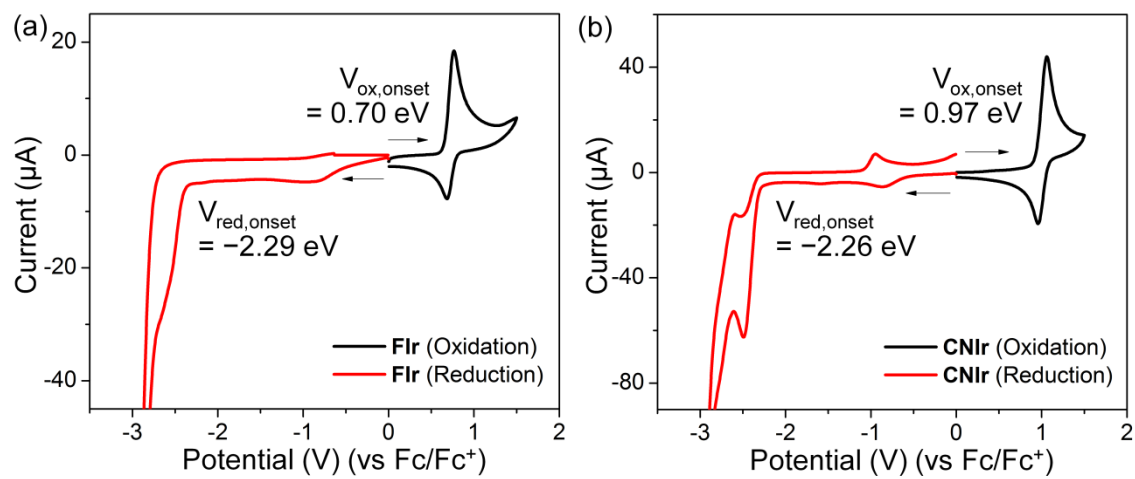


Fig. S5 Cyclic voltammograms (CV) of (a) **FIr** and (b) **CNIr** showing oxidation and reduction (5×10^{-4} M in DCM, scan rate: 100mV/s).

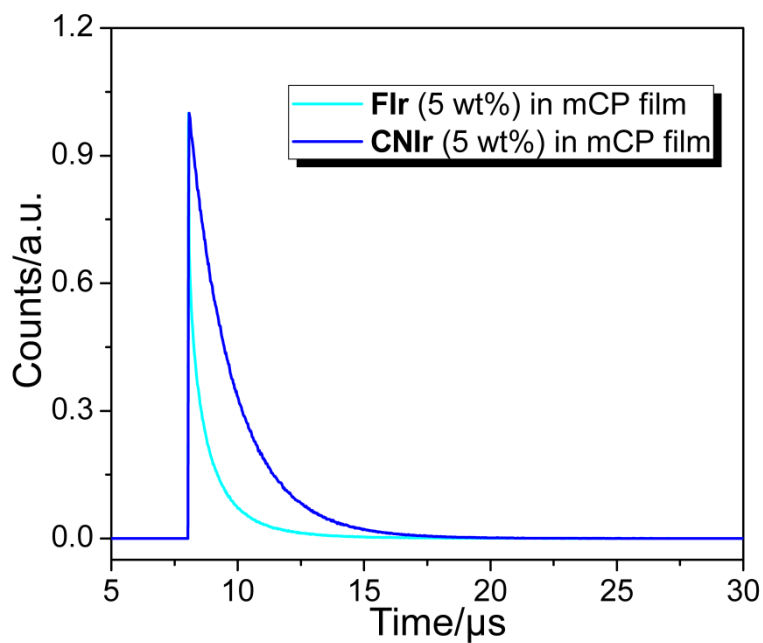


Fig. S6 Emission decay curves of **FIr** and **CNIr** (5 wt% doped in mCP film)

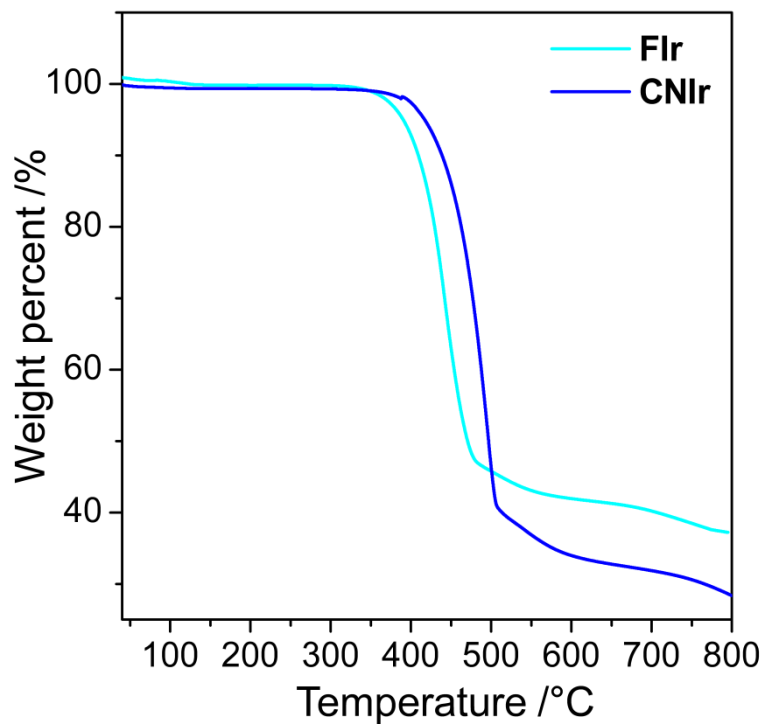


Fig. S7 TGA curves of **FIr** and **CNIr**

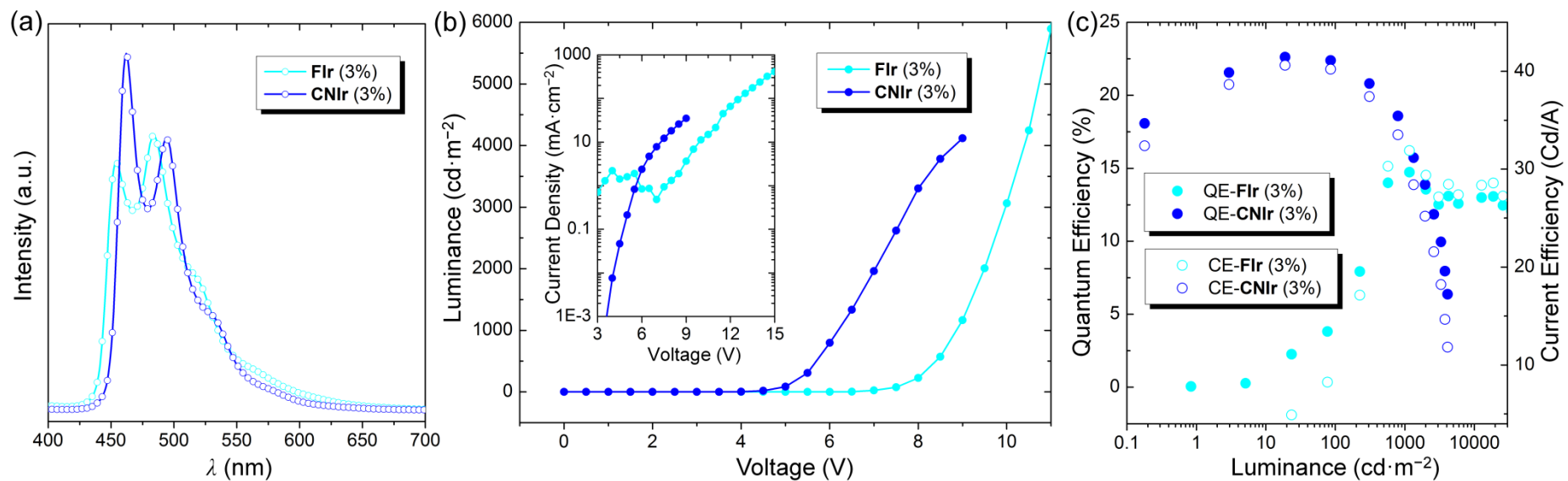


Fig. S8 (a) EL spectra of the OLEDs using **FIr** and **CNiR** (3%) with mCP, (b) luminance(L)–voltage(V) characteristics (the inset shows current density(J)–voltage(V) characteristics) and (c) external quantum efficiency–current efficiency–luminance(L) characteristics of the devices.

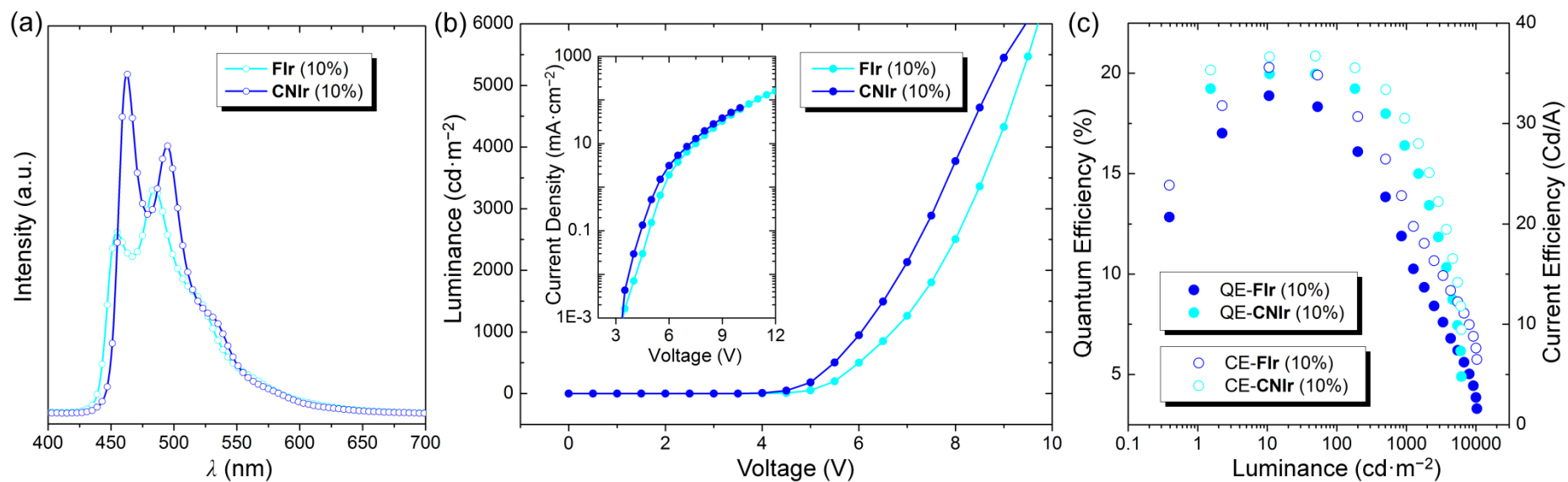


Fig. S9 (a) EL spectra of the OLEDs using **Flr** and **CNIr** (10%) with mCP, (b) luminance(L)–voltage(V) characteristics (the inset shows current density(J)–voltage(V) characteristics) and (c) external quantum efficiency–current efficiency–luminance(L) characteristics of the devices.

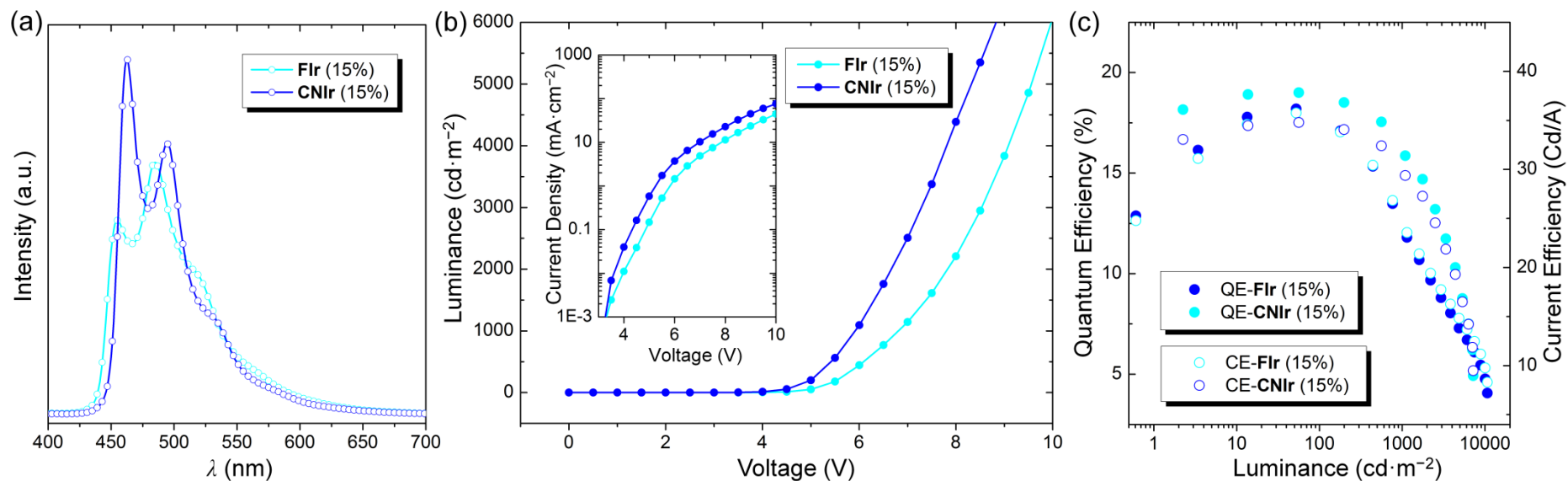


Fig. S10 (a) EL spectra of the OLEDs using **FIr** and **CNiR** (15%) with mCP, (b) luminance(L)–voltage(V) characteristics (the inset shows current density(J)–voltage(V) characteristics) and (c) external quantum efficiency–current efficiency–luminance(L) characteristics of the devices.

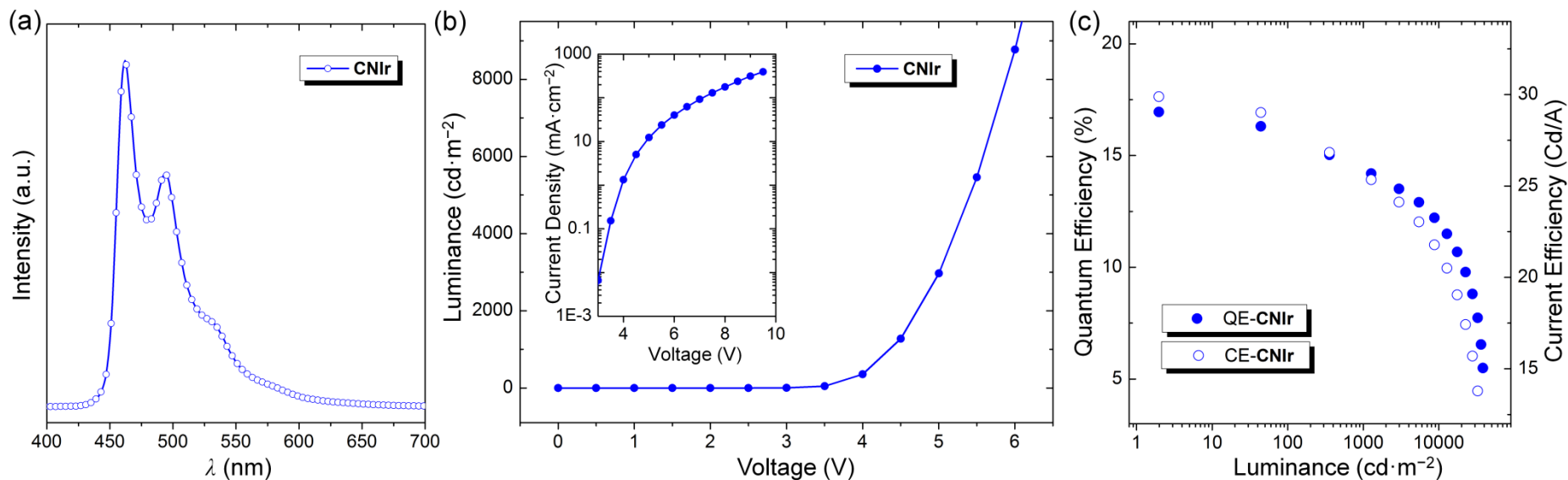


Fig. S11 (a) EL spectra, (b) luminance(L)–voltage(V) characteristics (the inset shows current density(J)–voltage(V) characteristics) and (c) external quantum efficiency–current efficiency–luminance(L) characteristics of the **CNIr** based device structure: ITO (50 nm)/BPBPA:HATCN (40 nm:30 wt%)/BPBPA (10 nm)/PCZAC (10 nm)/(mCBP:DBFTrz):**CNIr** ((50:50%):20 wt%) (30 nm)/DBFTrz (5 nm)/ZADN (20 nm)/LiF (1.5 nm)/Al (200 nm).